Mixed-Integer SDP Relaxation-based Volt/Var Optimization for Unbalanced Distribution Systems

Ibrahim Alsaleh*, Lingling Fan‡, Minyue Ma§
Electrical Engineering Department, University of South Florida
Tampa, FL 33620, USA
Email: *ialsaleh@mail.usf.edu, ‡linglingfan@usf.edu, §minyuema@mail.usf.edu

***Abstract*—This paper aims to conduct volt/var optimization for unbalanced distribution systems considering discrete tap changers, such as voltage regulators (VRs). There are two challenges to tackle this mixed-integer nonlinear optimization problem, namely, the difficulty to judge the quality of the solution and the lack of an effective solver. In this paper, we tackle both challenges. A sparse convex relaxation of branch flow model for multiphase distribution systems is adopted for the underlying optimal power flow problem. The overall problem becomes a mixed-integer semidefinite programming (MISDP) problem. Further, an effective generalized Benders decomposition (GBD) algorithm is developed in this paper to solve the problem. Bound-tightening technique is employed in this research to reduce the search region of the main problem, which renders a significantly faster convergence. Numerical tests on an IEEE 37-bus system demonstrate the convergence of the GBD and success in finding a global optimal setting of VR taps while abiding by the system's constraints.**

***Index Terms*—Voltage regulators, multiphase systems, generalized Benders decomposition, semidefinite programming**

I. Introduction

Volt/var optimization for distribution systems is a challenging problem. There are two modeling challenges: multiphase consideration and discrete control device consideration. Discrete control devices include voltage regulators (VRs), online load tap changers (OLTC), and switched capacitors. Simplification, such as single-phase treatment [1] and omission of discrete devices [2], is usually adopted.

The literature therein has endeavored various models to consider the two aspects. [3] uses a mixed-integer nonlinear program (MINLP) to determine the optimal tap setting in a multiphase OPF problem, while [4] builds an exact MIP-based VR model applicable to convex relaxation of branch flow-based power flow for single-phase systems only. It was then used in [5] to solve a simplified three-phase model where mutual impedances are ignored and quadratic loss terms are linearized. Further, [6] and [7] use an approximated VR model in which the tap ratios are relaxed, which recasts the primary-to-secondary voltage relationship as inequality constraints. Although simple, the arbitrariness of secondary-side phase angles that stems from this approximation generates rank-2 solutions for multiphase systems. In response, [6] proposed to tighten the solution by placing a tunable resistance between the sides of the ideal transformer.

Thus far, the emulation of discrete tap switching has not been tackled for the convex multiphase OPF models. The goal of this paper is to adequately model volt/var optimization for multiphase system and with VR considered. We first adopt the sparse semidefinite programming (SDP) relaxation-based branch flow model (BFM) proposed by Gan and Low [8], whose solutions has been shown to be tight for standard IEEE and other feeder tests. Compared to [9], the SDP-relaxed BFM has a lower-dimension SDP matrix for each line. We formulate a mixed-integer SDP problem and develop an efficient solver based on generalized Bender's decomposition (GBD). The following summarizes the contributions of this work:

1) The VR is incorporated into the SDP-relaxed BFM, whose variable structure is exploited to maintain the angle difference between the primary and secondary sides. If the OPF is rank-1, the tap setting is a global optimum.
2) The non-convexity in the variable edges caused by ratio bilinear terms are overcome by using Benders decomposition, where binaries are fixed in the subproblem (SP) and solved separately.
3) The iteration of the GBD is accelerated by bound tightening (BT) tap ratios in the master problem (MP). Bounds are calculated in optimization-based BT problems solved prior to the GBD.

The ensuing sections are organized as follows. Section II reviews the OPF problem and the VR model. Section III presents the standard GBD algorithm and its iteration. Further, the GBD algorithm with BT is discussed. Section IV demonstrates the effectiveness of the algorithms and conducts numerical tests on an IEEE 37-bus feeder with two VRs. Section V concludes the paper.

II. Problem Fromulation

A. OPF Model: SDP-based BFM

1) Notation: A radial distribution system can be modeled as a tree graph comprised of nodes and directed branch segments, $\mathcal{G}(\mathcal{N},\mathcal{E})$, where $\mathcal{N}$ and $\mathcal{E}$ correspond to the sets of buses and lines, respectively. $\mathcal{N}^+ = \mathcal{N} - \{0\}$ is the set of descent buses from the substation whose voltage magnitude is fixed, $V_0 = V_{\mathrm{nom}}$. A phase set of bus i is denoted as Φ_i, thus $\Phi \subseteq \{a, b, c\}$. Diagonal and off-diagonal phase elements are denoted as $\phi\phi$ and ϕ, respectively.

2) SDP-based BFM [8]:

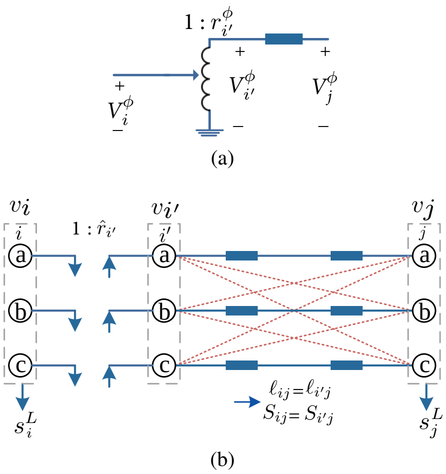

Fig. 1: (a) Per-phase tap-changing transformer model. (b) Variable representation in SDP-based BFM

Ohm's Law: For each branch $i \to j$

$$V_j = V_i - z_{ij} I_{ij} \tag{1}$$

where V_i, V_j, and $I_{ij} \in \mathbb{C}^{|\Phi_j|}$, while $z_{ij} \in \mathbb{C}^{|\Phi_j|\times|\Phi_j|}$. By multiplying both sides by their Hermitian transposes, and defining $v_i = V_i V_i^H$, $v_j = V_j V_j^H$, $S_{ij} = V_i I_{ij}^H$ and $\ell_i = I_{ij} I_{ij}^H$, then (1) can be re-written as

$$v_j = v_i - (S_{ij} z_{ij}^H + z_{ij} S_{ij}^H) + z_{ij}\ell_{ij} z_{ij}^H \quad \forall \ (i,j) \in \mathcal{E} \tag{2}$$

where v_i, v_j, ℓ_{ij}, and $S_{ij} \in \mathbb{C}^{|\Phi_j|\times|\Phi_j|}$ with diagonal entries of v_i, v_j and ℓ_{ij} as squared magnitudes and off-diagonal ones as mutual complex elements.

Power Balance: For each $i \to j \to k$, to interpret the power balance at j, (1) is multiplied by I_{ij}^H

$$V_j I_{ij}^H = V_i I_{ij}^H - z_{ij} I_{ij} I_{ij}^H \tag{3}$$

$$V_j \Big(\sum_{k:(j,k)\in\mathcal{E}} I_{jk}^H + (I_j^L)^H \Big) = S_{ij} - z_{ij}\ell_{ij} \tag{4}$$

where I_j^L is the load current at bus j. As a result, the power balance at bus j is the diagonal of (4), which is expressed as

$$\sum_{k:(j,k)\in\mathcal{E}} \mathrm{diag}(S_{jk}) + s_j^L = \mathrm{diag}(S_{ij} - z_i \ell_{ij}) \, \forall (i,j) \in \mathcal{E} \tag{5}$$

PSD and Rank-1 Matrix: To close the gap and set the relationship between actual electrical components and surrogate variables, the following positive and rank-1 matrix is defined

$$X_{ij} = \begin{bmatrix} V_i \\ I_{ij} \end{bmatrix} \begin{bmatrix} V_i \\ I_{ij} \end{bmatrix}^H = \begin{bmatrix} v_i & S_{ij} \\ S_{ij}^H & \ell_{ij} \end{bmatrix}$$

$$X_{ij} \succeq 0 \qquad \forall \ (i,j) \in \mathcal{E} \tag{6}$$

$$\mathrm{rank}(X_{ij}) = 1 \quad \forall \ (i,j) \in \mathcal{E} \tag{7}$$

Convexification: The rank-1 constraint (7) is removed from the set of constraints to arrive at a convex problem. The solution however should hold tight for each line. A tightness check will be conducted for the results in Section V.

Voltage Limits: $\pm 5\%$ of the nominal voltage are enforced as bounds on each element of the diagonal voltage squares.

$$\underline{V}^2 \leq \mathrm{diag}(v_i) \leq \overline{V}^2 \quad \forall \ i \in \mathcal{N}^+ \tag{8}$$

B. VR Model

Three-phase voltages are regulated by connecting three single-phase VRs. Fig. 1a shows a per-phase VR installed on $(i,j) \in \mathcal{E}$, which is an autotransformer with lumped leakage and line impedance. The VR incorporation into the OPF problem is approached by connecting the primary of an ideal transformer to bus i, and introducing a virtual bus to the system, $i' \in \mathcal{N}^+$, to represent the secondary side. Hence, an additional variable alluding to the secondary-side voltage is required.

The VR's per-phase ratio $r_{i'}^{\phi}$ can typically take 33 values from 90% to 110% with a $\Delta r_{i'} = 0.625\%$ ratio change per tap (± 16 and neutral positions). For simplicity, the per-phase ratio selection is modeled as in (9) with binary variables, $u_{i'} \in \mathbb{U}^{|M|\times|\Phi_{i'}|}$, where $M = 32$ and R_m is the discrete tap ratio at tap m. The sum of $u_{i'}$ to 1 yields a single ratio.

$$r_{i'}^{\phi} = \sum_{m=0}^{M} \underbrace{(0.9 + \Delta r_{i'} \times m)}_{R_m} u_{i',m}^{\phi} = R^T u_{i'}^{\phi} \tag{9a}$$

$$\sum_{m=0}^{M} u_{i',m}^{\phi} = 1 \quad \forall \phi \in \Phi, i' \in \mathcal{N}^+ \tag{9b}$$

It should be noted that the voltage phase angles in the multi-phase BFM are implicitly formed by the off-diagonal complex entries, whereas diagonal entries represent their squared voltage magnitudes (real values). Therefore, the secondary-side matrix voltage variable is formulated as

$$v_{i'} = (r_{i'} r_{i'}^T) \odot v_i = \hat{r}_{i'} \odot v_i \quad \forall i' \in \mathcal{N}^+ \tag{10}$$

where $\odot$ is an element-wise multiplication operator. Thus

$$\hat{r}_{i'} = \begin{bmatrix} (r_{i'}^a)^2 & r_{i'}^a r_{i'}^b & r_{i'}^a r_{i'}^c \\ r_{i'}^b r_{i'}^a & (r_{i'}^b)^2 & r_{i'}^b r_{i'}^c \\ r_{i'}^c r_{i'}^a & r_{i'}^c r_{i'}^b & (r_{i'}^c)^2 \end{bmatrix}$$

Because $\sum_m u_{i',m}^{\phi} = 1$ and there is only one $u_{i',m}$ being 1 with the rest being 0, also $(u_{i',m}^{\phi})^2 = u_{i',m}^{\phi}$, then the diagonal element $(r_{i'}^{\phi})^2 = (R^T u_{i'}^{\phi})^2$ can be expressed as $\sum_m R_m^2 u_{i',m}^{\phi} = W^T u_{i'}^{\phi}$ (where W is a column vector with R_m^2 as elements).

C. Overall Optimization Problem

The rank-relaxed SDP-based OPF problem aims at minimizing the system's power import from the substation, and flattening the voltage profile.

$$\min_{v,\ell,S,u} \ \mathrm{Tr}\big(\mathrm{Re}(S_{\mathrm{sub}}) + \mathrm{Im}(S_{\mathrm{sub}})\big) + \alpha \sum_{i\in\mathcal{N}^+} \sum_{\phi\in\Phi} |v_i^{\phi\phi} - V_{\mathrm{nom}}^2| \tag{11a}$$

$$\text{s. t.} \quad v_0 = V_{\mathrm{nom}} V_{\mathrm{nom}}^H \tag{11b}$$

$$(2), (5), (6), (8), (9b), (10) \tag{11c}$$

III. Generalized Benders Decomposition

In this section, we apply the GBD [10], an extended version of [11], to decouple and solve the problem iteratively, thereby avoiding the non-convexity caused by binary-variable multiplication in (10). In each iteration, the binary variable solution to the master problem is passed to the subproblem. The subproblem will be solved and an optimality cut will be created for the master problem. If the master renders the subproblem infeasible, the subproblem will be reformulated and a feasibility cut be created.

A. Standard GBD

We denote continuous and binary variables as $x = \{v, S, \ell\} \in \mathbb{X}$ and $u \in \mathbb{U}$, respectively.

1) Subproblem (SP): The subproblem corresponding to the convex problem in the x-space only is succinctly written as following. It is the OPF problem with $\hat{u}$ obtained from the MP.

$$\begin{aligned} &\textbf{SP}: \theta_{\text{ub}} = \min_{x} \quad F(x) \\ &\text{s. t.} \quad v_{i'} = \hat{r}_{i'} \odot v_i, \quad x \in \mathbb{X} \end{aligned} \tag{12}$$

If the SP has a solution for $\hat{u}$, the optimal objective to SP is an upper bound to the original problem, notated as θ_{ub}. It also provides optimal Lagrangian multipliers $\lambda \in \mathbb{R}^{|\Phi_{i'}|}$ associated with the real diagonal of the secondary-side voltage, diag$(v_{i'})$.

Note for each VR, based on (10), there are 9 equality constraints. When creating cuts, only three constraints related to the diagonal components are considered:

$$v_{i'}^{\phi\phi} = W^T u_{i'}^{\phi} v_i^{\phi\phi} : \text{dual variable } \lambda_{i'}^{\phi,k}.$$

This consideration simplifies the cuts creating procedure. In addition, when $v_{i'}$ and v_i are rank-1, enforcing the diagonal elements of the left and right matrices equal guarantees the rest 6 equality constraints being satisfied.

2) Feasibility-Check Problem (FCP): If $\hat{u}$ renders SP infeasible, SP is reformulated as FCP in (13) to guarantee that a feasible solution exists for any u-value. The solution of this is used to generate a feasibility cut and to ensure the MP avoids this particular combination of $\hat{u}$. Hence, a slack matrix variable w, serving to relax taps causing infeasibility, is minimized, and introduced to each equality constraint pertaining to the tap ratio violation.

$$\begin{aligned} &\textbf{FCP}: \theta_{\text{fc}} = \min_{x,w} \quad \text{Trace}(w) \\ &\text{s. t.} \quad v_{i'} = \hat{r}_{i'} \odot v_i + w, \quad w \succeq 0, \quad x \in \mathbb{X} \end{aligned} \tag{13}$$

where Trace(w) is minimized, and diag(w) is constrained to be non-negative. The optimal objective of (13), θ_{fc}, and Lagrangian multipliers $\mu \in \mathbb{R}^{|\Phi_{i'}|}$ associated with the diagonal of equality constraint in (13) are then utilized to create a feasibility cut.

Algorithm 1: Optimal Tap Setting Using GBD

Pick any $\hat{u} \in \mathbb{U}$. Initialize $\theta_{\text{lb}}^0 = -\infty$ and $\theta_{\text{ub}}^0 = \infty$
while $\epsilon \leq |\theta_{\text{ub}}^{n_k} - \theta_{\text{lb}}^{n_k}|$ **do**
  solve the SP and find the dual related to u
  if solution is bounded (finite and feasible) **then**
    increase n_k by 1, and update $\theta_{\text{ub}}^{n_k}$ and λ^{n_k}
  else
    solve FCP
    increase n_l by 1, and update $\theta_{\text{fc}}^{n_l}$ and μ^{n_l}
  end if
  solve MP, update $\theta_{\text{lb}}^{n_k}$ and $\hat{u}$
end while

---

3) Master Problem (MP): In association with solutions to (12) and (13), the MP is formulated with constraints on binary variables, and optimality and feasibility cuts generated from the subproblems at each iteration.

$$\begin{aligned} &\textbf{MP}: \theta_{\text{lb}} = \min_{u,\eta} \quad \eta \\ &\eta \geq \theta_{\text{ub}}^k + \sum_{i' \in \mathcal{N}^+} \sum_{\phi \in \Phi} \lambda_{i'}^{\phi,k} W^T \big(u_{i'}^{\phi} - \hat{u}_{i'}^{\phi,k}\big) \;\; k = 1, \cdots, n_k \\ &0 \geq \theta_{\text{fc}}^l + \sum_{i' \in \mathcal{N}^+} \sum_{\phi \in \Phi} \mu_{i'}^{\phi,l} W^T \big(u_{i'}^{\phi} - \hat{u}_{i'}^{\phi,l}\big) \;\; l = 1, \cdots, n_l \\ &\sum_{m=0}^{M} u_{i',m}^{\phi} = 1 \quad \forall \phi \in \Phi, i' \in \mathcal{N}^+ \end{aligned} \tag{14}$$

The optimal objective, θ_{lb}, provides the lower bound. The problems iterate until their objectives meet a pre-defined tolerance, ϵ.

B. GBD with Bound Tightening

As the secondary voltage in the SP is constrained within bounds, the SP's infeasibility occurs when the MP renders a tap position that results in the secondary voltage exceeding the upper bound or falling below the lower one. In the standard GBD, FCP should be formulated to create a cut whenever the SP is infeasible. This however increases the iterations, as a feasibility cut is created each time the MP visits an infeasible tap ratio at a certain phase. Motivated by the work in [12], a method is proposed in which feasible ratios are reckoned a $priori$, and used to constrain tap ratios in the MP.

1) Bound Tightening Problems (BT): The original problem is re-formulated such that the secondary voltage is bounded by the primary voltage multiplied by ratio limits. The objective function is to minimize (maximize) the secondary voltage to determine the ratios' lower (upper) bounds, $\underline{R}_i$ ($\overline{R}_i$) $\in \mathbb{R}^{|\Phi_{i'}|}$.

$$\textbf{BT} := \min_x (\text{or} \max_x) \quad \sum_{i' \in \mathcal{N}^+} \sum_{\phi \in \Phi} v_{i'}^{\phi\phi} \tag{15a}$$

$$0.9^2 v_i^{\phi\phi} \leq v_{i'}^{\phi\phi} \leq 1.1^2 v_i^{\phi\phi} \quad \forall \phi \in \Phi, i' \in \mathcal{N}^+ \tag{15b}$$

$$v_{i'}^{\phi} = v_i^{\phi} \quad \forall \phi \in \Phi, i' \in \mathcal{N}^+ \tag{15c}$$

$$(2), (5), (6), (8), (11\text{b}) \tag{15d}$$

Algorithm 2: Optimal Tap Setting Using GBD with BT

solve BT problems and compute $\underline{R}$ and $\overline{R}$
Pick any $\hat{u} \in \mathbb{U}$. Initialize $\theta_{\text{lb}}^0 = -\infty$ and $\theta_{\text{ub}}^0 = \infty$
while $\epsilon \leq |\theta_{\text{ub}}^{n_k} - \theta_{\text{lb}}^{n_k}|$ **do**
  solve the SP and find the dual related to u
  increase n_k by 1, and update $\theta_{\text{ub}}^{n_k}$ and λ^{n_k}
  solve MP'($\underline{R}, \overline{R}$)
  update $\theta_{\text{lb}}^{n_k}$ and $\hat{u}$
end while

Ratio bounds are computed as $\underline{R_{i'}}(\overline{R}_{i'}) = \text{diag}(v_{i'}) \oslash \text{diag}(v_i)$. $\oslash$ is an element-wise division operator.

2) Master Problem (MP'): By constraining tap ratios with $\underline{R_{i'}}$ and $\overline{R}_{i'}$, the feasibility-cut constraints are omitted in MP', as the solution to (16) will always make the subproblem feasible.

$$\begin{aligned} &\textbf{MP'} := \min_{u,\eta} \quad \eta \\ &\eta \geq \theta_{\text{ub}}^k + \sum_{i' \in \mathcal{N}^+} \sum_{\phi \in \Phi} \lambda_{i'}^{\phi,k} W^T \left(u_{i'}^{\phi} - \hat{u}_{i'}^{\phi,k}\right) \;\; k = 1, 2, \ldots, n_k \\ &\sum_{m=0}^{M} u_{i',m}^{\phi} = 1, \quad \underline{R}_{i'} \leq W^T u_{i'}^{\phi} \leq \overline{R}_{i'} \quad \forall \phi \in \Phi, i' \in \mathcal{N}^+ \end{aligned} \tag{16}$$

IV. Numerical Case Studies

Fig. 2 depicts the modified IEEE 37-bus feeder, an actual feeder with unbalanced loads and lines. All lines are three-phase configured. Loads at buses 9, 10, 12, 32, and 33 are increased by 30% to examine the VRs' ability to compensate for voltages of heavy-loaded and remote buses that tend to fall below 0.95 pu during peak. The peak demand becomes 2.906 MVA with 0.9 PF lagging. Two VRs, each with 33 levels and a turns ratio varying from 0.9 to 1.1, are installed on two lines.

For both algorithms, the simulations are implemented in MATLAB using CVX toolbox [13]. The SDP-based SP, FCP, and BT are solved by Mosek solver [14], while the IP-based MP and MP' are solved by Gurobi solver [15]. The tolerance, ϵ, is chosen to be 1e−6.

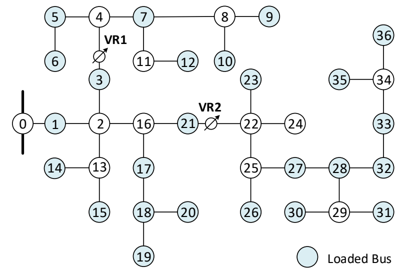

Fig. 2: Modified IEEE 37-bus feeder.

A. Optimal Tap Setting

Algorithm 2 is carried out with different penalties and five loading assumptions.

1) Without Flatness Penalty: Setting α to 0, the algorithm is tested with the first objective term. The results in Table I indicate that VRs tap high, even though lower tap ratios are presumably sufficient. The reason is that high voltages minimize system losses; therefore, the minimum total power drawn from the substation is needed. However, higher voltages result in higher energy consumption of voltage-dependent loads. Fig. 3a shows the voltage profile at 100% loading.

2) With Flatness Penalty: When the voltage flatness is considered ($\alpha = 1$), optimal VR tap ratios are closer to unity (neutral position) in an effort to achieve the trade-off between the two objectives. Consequently, a flatter profile is obtained as seen in Fig. 3b.

B. Relaxation Tightness

The ratio between the second-dominant eigenvalue and the dominant eigenvalue, $|\text{eig}_2/\text{eig}_1|$ where $|\text{eig}_1| \geq |\text{eig}_2| \geq 0$, of the SDP matrices measures the proximity to rank-1, and thus the solution tightness. Because the per-loading maximum ratio over all lines satisfies a sufficiently small value, as tabulated in the last column of Table I, the relaxation is deemed exact.

C. Standard GBD vs GBD with BT

Fig. 4a-4c illustrate a comparison of the two algorithms in the number of iterations and computation time over 10

TABLE I: Numerical Results for The Proposed Method

System Loading	Flatness Penalty α	Sub. Power (pu)		Opt. Ratio of VR1			Opt. Ratio of VR2			Sys. Voltage (pu)		Tightness
		P	Q	*A*	*B*	*C*	*A*	*B*	*C*	maximum	minimum	$\max(\lvert\frac{\text{eig}_2}{\text{eig}_1}\rvert)$
100%	0	2.6949	1.3073	1.0687	1.0687	1.0687	1.0812	1.075	1.0812	1.0485	0.9658	5.9846e-07
	1	2.6963	1.3079	1.025	1.0312	1.0312	1.05	1.0375	1.05	1.0159	0.9658	9.5939e-09
80%	0	2.1417	1.0408	1.0625	1.0625	1.0687	1.075	1.0687	1.075	1.0495	0.9729	3.3001e-07
	1	2.1427	1.0412	1.0187	1.0187	1.025	1.0375	1.025	1.0375	1.0132	0.9729	1.1361e-08
60%	0	1.5959	0.7769	1.0562	1.0562	1.0625	1.0687	1.0625	1.0687	1.0483	0.9798	1.2951e-07
	1	1.5965	0.7772	1.0125	1.0187	1.0187	1.025	1.0187	1.025	1.0072	0.9798	2.7155e-09
40%	0	1.0571	0.5155	1.0562	1.0562	1.0562	1.0625	1.0562	1.0625	1.0491	0.9866	3.0656e-09
	1	1.0574	0.5156	1.0062	1.0125	1.0125	1.0187	1.0125	1.0187	1.0059	0.9866	3.7393e-08
20%	0	0.5253	0.2566	1.05	1.05	1.05	1.05	1.05	1.05	1.0496	0.9934	2.1161e-08
	1	0.5254	0.2566	1	1	1.0062	1.0062	1.0062	1.0062	1.0018	0.9925	2.9842e-09

loading conditions. While the two algorithms result in equivalent objective values, and thus tap ratios of VR1 and VR2, it is obvious that the GBD along with BT strategy has a computational advantage over that of the standard one with 18 iterations and 51.2 s on average.

Fig. 4d shows the iterations of algorithm 1 and 2 for 100% loading, where 15 and -15 correspond to infinite values. Bound tightening technique can greatly speed up convergence.

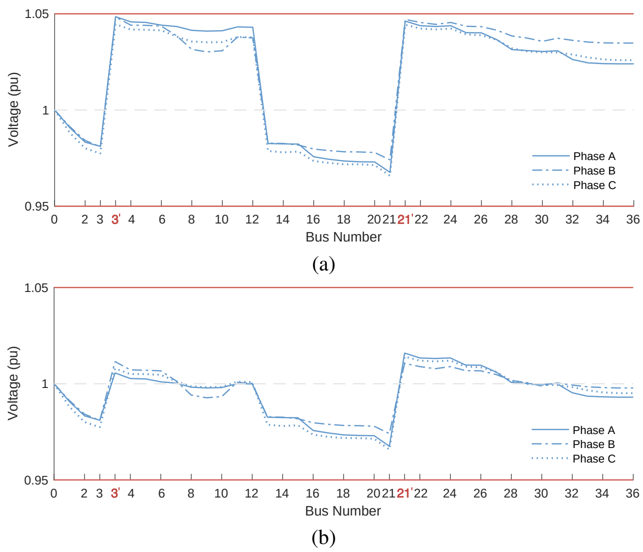

Fig. 3: Voltages during 100% loading (a) $\alpha = 0$, (b) $\alpha = 1$.

V. Conclusion

In this paper, an optimal tap setting for VRs, in a convex multiphase AC OPF framework, was proposed. The discrete nature of the taps present in the primary-to-secondary voltage constraints renders the overall problem non-convex. Therefore, GBD was applied to solve the mixed-integer SDP problem. In addition, bound-tightening problems were proposed, whose solution is used to enhance the computation of the GBD. The results demonstrated the applicability of this method in regulating nodal voltages with multiple loading conditions. Given that the algorithm proposed yields tight SDP solutions, future work will utilize these promising results to develop a more comprehensive volt/var optimization for distribution systems.

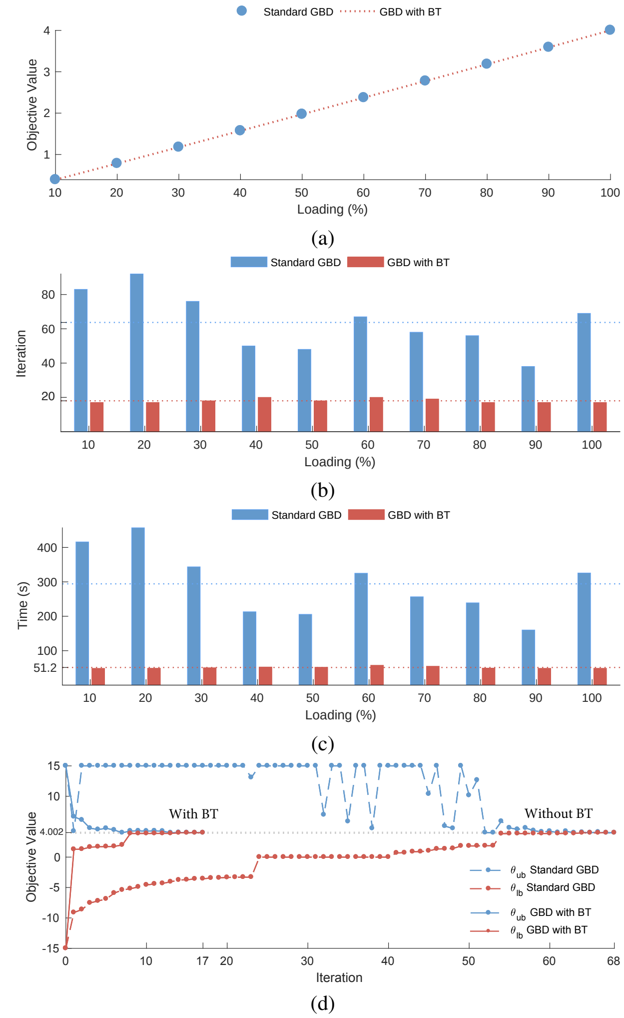

Fig. 4: (a) Objective values, (b) iterations, and (c) computation time of algorithm 1 and 2 with 10 loading conditions. (d) Upper and lower values of algorithm 1 and 2 for 100% loading.

References

[1] I. Alsaleh, L. Fan, and H. G. Aghamolki, "Volt/var optimization with minimum equipment operation under high pv penetration," in *North American Power Symposium*. IEEE, 2018, pp. 1–6.

[2] I. Alsaleh and L. Fan, "Distribution locational marginal pricing (dlmp) for multiphase systems," in *North American Power Symposium*. IEEE, 2018, pp. 1–6.

[3] S. Paudyal, C. A. Cañizares, and K. Bhattacharya, "Optimal operation of distribution feeders in smart grids," *IEEE Transactions on Industrial Electronics*, vol. 58, no. 10, pp. 4495–4503, 2011.

[4] W. Wu, Z. Tian, and B. Zhang, "An exact linearization method for oltc of transformer in branch flow model," *IEEE Transactions on Power Systems*, vol. 32, no. 3, pp. 2475–2476, 2017.

[5] X. Chen, W. Wu, and B. Zhang, "Robust capacity assessment of distributed generation in unbalanced distribution networks incorporating anm techniques," *IEEE Transactions on Sustainable Energy*, vol. 9, no. 2, pp. 651–663, 2018.

[6] B. A. Robbins, H. Zhu, and A. D. Domínguez-García, "Optimal tap setting of voltage regulation transformers in unbalanced distribution systems," *IEEE Transactions on Power Systems*, vol. 31, no. 1, pp. 256–267, 2016.

[7] M. Bazrafshan, N. Gatsis, and H. Zhu, "Optimal tap selection of step-voltage regulators in multi-phase distribution networks," in *2018 Power Systems Computation Conference (PSCC)*. IEEE, 2018, pp. 1–7.

[8] L. Gan and S. H. Low, "Convex relaxations and linear approximation for optimal power flow in multiphase radial networks," in *Power Systems Computation Conference (PSCC), 2014*. IEEE, 2014, pp. 1–9.

[9] E. Dall'Anese, H. Zhu, and G. B. Giannakis, "Distributed optimal power flow for smart microgrids." *IEEE Trans. Smart Grid*, vol. 4, no. 3, pp. 1464–1475, 2013.

[10] A. M. Geoffrion, "Generalized benders decomposition," *Journal of optimization theory and applications*, vol. 10, no. 4, pp. 237–260, 1972.

[11] J. F. Benders, "Partitioning procedures for solving mixed-variables programming problems," *Numerische mathematik*, vol. 4, no. 1, pp. 238–252, 1962.

[12] M. Bynum, A. Castillo, J.-P. Watson, and C. D. Laird, "Tightening mccormick relaxations toward global solution of the acopf problem," *IEEE Transactions on Power Systems*, 2018.

[13] M. Grant, S. Boyd, and Y. Ye, "Cvx: Matlab software for disciplined convex programming," 2008.

[14] A. Mosek, "The mosek optimization toolbox for matlab manual," 2015.

[15] G. Optimization, "Gurobi optimizer reference manual, 2015," *URL: http://www. gurobi. com*, 2014.